Optimal Flux Barrier Design of Interior Permanent Magnet Motor for Torque Ripple Reduction under Stress Constraint

Seunggyun Park, Seungjae Min, and Jung-Pyo Hong
Department of Automotive Engineering, Hanyang University
17 Haengdang-dong, Sungdong-gu, Seoul, 133-791, Korea
psgsky@gmail.com, seungjae@hanyang.ac.kr, hongjp@hanyang.ac.kr

Abstract — The flux barrier in Interior Permanent Magnet(IPM) motor plays an important role to maximize the magnetic performance and the structural strength becomes an issue in the high speed applications. In this paper, the harmonics of the tangential magnetic force in the teeth is considered to reduce the torque ripple and the stress constraint is employed to ensure the mechanical performance. The configuration of the flux barrier is represented by the level-set function and the optimization problem is solved by the augmented Lagrangian method. The practical example shows that the optimal flux barrier design for the torque ripple reduction can be achieved with the specified the allowable stress and the amount of ferromagnetic material.

I. INTRODUCTION

Interior Permanent Magnet(IPM) motor has widely used in many applications because of high efficiency and power density. However, high torque ripple caused by the difference of magnetic resistance between d and q-axis has influence on vibration and noise. The two main approaches to reduce the torque ripple are based on the control of the current waveform and the configuration change of stator and/or rotor. Regarding on the rotor design, the flux barrier serves as controlling the flux path and plays an important role for torque ripple reduction. In the design of a flux barrier, the variation of bridge thickness produces the effects on both the magnetic and the mechanical performance [1]. The mechanical stress analysis is generally separated from the magnetic field analysis and it is performed to check the strength of the bridge after the flux barrier design [2]-[3]. Even if the mechanical strength is considered with the magnetic field analysis simultaneously, they used the parametric model [4].

In this paper, the torque ripple is reduced by considering the harmonics of the tangential magnetic force in the teeth and the mechanical strength is maintained by employing the stress constraint in the level-set based topology optimization [5].

II. MAGNETIC AND MECHANICAL PERFORMANCE

A. Torque Ripple Reduction

Since the tangential magnetic force in the teeth is directly related to the torque calculation, harmonics analysis is performed. It turned out that the harmonics of the tangential magnetic force are overlapped and amplified at the specific harmonics which result in the torque ripple. The specific *j*-th harmonics can be found that the value of *j* multiplied by the ratio of the number of the pole to the number of the slot becomes the integer multiples. The ideal tangential magnetic force profile can be obtained by removing the specific *j*-th harmonics.

B. Stress Constraint

IPM motor has the critical mechanical stress caused by centrifugal force when it is operated at the high speed and it can deform or break the bridge [4]. In order to ensure the structural strength, the stress constraint is considered. Since the stress is the local quantity in the structure, a large number of constraints are generally required to formulate the optimization problem. To deal with the local nature of the constraint effectively, a single integrated stress constraint that approximates the maximum stress is introduced to resolve the complication [6]-[7]. The p-norm measure for the global stress constraint can be defined by

$$\sigma_{PN} = \left(\sum_{i=1}^{n} \sigma_i^P \right)^{1/P} \le \sigma_{\max} \tag{1}$$

where n represents the number of elements.

III. PROBLEM FORMULATION

The level-set function(ϕ) represents the structural boundaries of the flux barrier and the objective function is defined to minimize the difference between the tangential magnetic force wave(F_t) and the target wave(F_t^*) which eliminates the amplified harmonics and maximize the offset value(F_{avg}) to increase the average torque. The volume constraint is specified by the amount of ferromagnetic material($V_{\max}$) distributed in the design domain(Ω_d) and the stress constraint is imposed. Therefore, the new level-set based topology optimization problem can be formulated as

$$\begin{aligned} &\text{find } \{x \mid \phi(x) = 0\} \text{ to} \\ &\text{minimize } f = \left(\frac{F_t - F_t^*}{F_{avg}} \right)^2 \\ &\text{subject to } g_1 = \sum_{\Omega_d} H(\phi(x)) - V_{\max} \le 0 \\ &\qquad g_2 = \left(\sum_{\Omega_d} \left(\sigma(\phi(x)) \right)^p \right)^{1/p} - \sigma_{\max} \le 0 \end{aligned} \tag{2}$$

where $H(\phi(x))$ is the Heaviside.

In order to obtain the solution of the constrained problem, the augmented Lagrangian method is employed. The normal velocity of the level-set boundary can be derived from both KKT condition and the convergence criteria of the level-set equation as

$$V_n = \frac{df}{d\phi} + \sum_{i=1}^{2} \left(\left(\lambda_i + r_i g_i(\phi) \right) \frac{dg_i}{d\phi} \right) \tag{3}$$

where λ_i represents the Lagrange multiplier and r_i the penalty factor. During optimization process, the Lagrange multipliers are updated by

$$\lambda_{i,k+1} = \lambda_{i,k} + r_i g_i(\phi) \tag{4}$$

where k is the number of iteration.

IV. DESIGN EXAMPLE

The cross section of V-type IPM motor where the specifications are summarized in Table I and the design domain where the flux barrier is created are shown in Fig. 1. The maximum volume is constrained for 35% of the design domain and the maximum value of von-Mises stress is specified by 100[N/mm^2] considering the safety factor of 3 for the ferromagnetic material (blue color) when it is operated at the high speed. Fig. 2(a) shows the optimal configuration of the flux barrier without considering the stress constraint and the maximum stress with much higher value than the allowable stress can be found at the corner of the narrow bridge. Incorporating with the stress constraint, the ferromagnetic material tends to be distributed at the bridge to lower the maximum stress in Fig. 2(b), and it attempts to tradeoff between the magnetic and the mechanical performance. Fig. 3 compares the torque profiles for each case and it is noted that the thickness of bridge has influence on the average torque because the flux leakage becomes larger as it is increased and the distance between the bridge and the magnet becomes larger to get the sinusoidal flux density distribution in the air gap. Fig. 4 illustrates the iteration histories of the global stress and the practical importance of the stress constraint.

Finally it is confirmed that the proposed method can provide the flexible tool to design the optimal flux barrier of IPM motor satisfying both the torque performance and the mechanical strength summarized in Table II.

TABLE I. SPECIFICATIONS OF V-TYPE IPM MOTOR

Number of poles / slots / phases		12 / 18 / 3
Diameter [mm]	Stator	292
	Rotor	204.8
Stack length [mm]		85
Core material		RM14
Remanent flux density of magnet [T]		1.103
Maximum speed [rpm]		3400
Young's modulus [N/mm^2] / Poisson ratio		2.05e5 / 0.3
Material density[kg/m^3]		7850
Allowable stress of the electric steel [N/mm^2]		363

TABLE II. PERFORMANCE COMPARISON

	Torque ripple[%]	Average torque[Nm]	Maximum stress[N/mm^2]
Initial design	231.6	53.2	57.7
Without stress constraint	43.1	53.4	231.5
With stress constraint	43.3	50.4	94.4

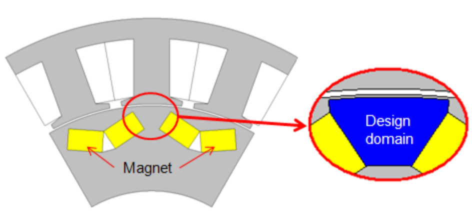

Fig. 1. Cross section of the V-type IPM motor and design domain

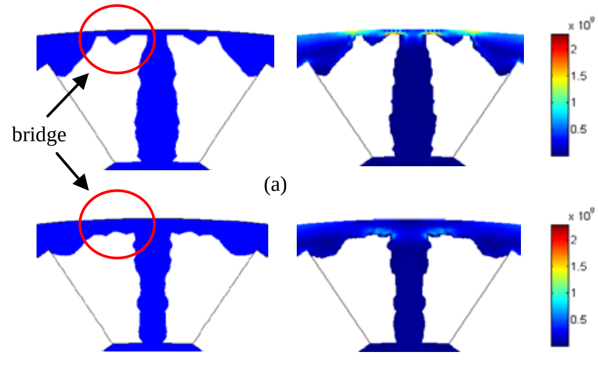

Fig. 2. Optimal flux barrier design and stress distribution: (a) without stress constraint (b) with stress constraint

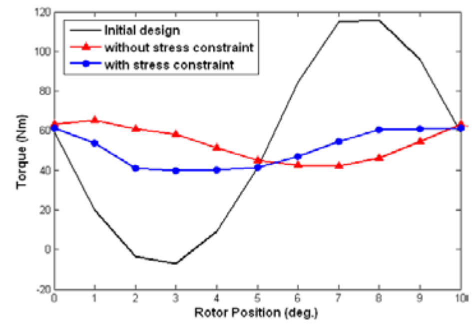

Fig. 3. Torque profile

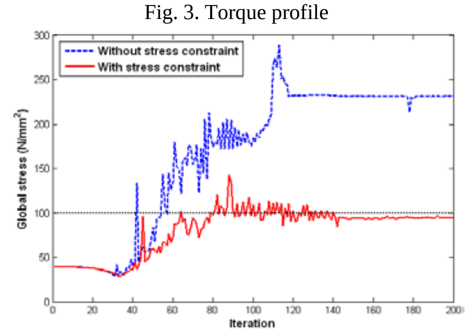

Fig. 4. Iteration history of global stress

V. REFERENCES

[1] E. Lovelace, T. Jahns, T. Keim and J. Lang, “Mechanical design considerations for conventionally laminated, high-speed, interior PM synchronous machine rotors,” *IEEE Trans. on Industry Applications*, vol.40, no.3, pp. 806-812, 2004.

[2] S. Kim and G. Lee, C. Lee and J. Hong, “Design and experimental verification of an interior permanent magnet motor for high speed machines,” *Trans. KIEE*, vol.59, no.2, pp. 306-310, 2010.

[3] J. Kim, S. Kwak, S. Cho, H. Jung, T. Chung and S. Jung, “Optimization of multilayer buried magnet synchronous machine combined with stress and thermal analysis,” *IEEE Trans. on Magn.*, vol.42, no.4, pp. 1023-1026, 2006.

[4] J. Seo, S. Kim and H. Jung, “Rotor-design strategy of IPMSM for 42V Integrated starter generator,” *IEEE Trans. on Magn.*, vol.46, no.6, pp. 2458-2461, 2010.

[5] J. Kwack, S. Min and J. Hong, "Optimal stator design of interior permanent magnet motor to reduce torque ripple using the level set method,” *IEEE Trans. on Magn.*, vol.46, no.6, pp. 2108-2111, 2010.

[6] J. Paris, F. Navarrina, I. Colominas and M. Casteleiro, “Topology optimization of continuum structures with local and global stress constraints,” *Struct. Multidisc. Optim*, vol.39, no.4, pp. 419-437, 2009.

[7] C. Le, J. Norato, T. Bruns, C. Ha and D. Tortorelli, "Stress-based topology optimization for continua,” *Struct. Multidisc. Optim.*, vol.41, no.4, pp. 605-620, 2010.